MIF produced by bone marrow-derived macrophages contributes to teratoma progression after embryonic stem cell transplantation

Xi Wang[1,8], **Jianqing Fan**[2], **Lin Leng**[3], **Kai Cao**[1], **Zhaoxia Duan**[1,9], **Tianxiang Chen**[1,6], **Xijing Zhang**[4], **Changshun Shao**[5], **Iman Tadmori**[1], **Tianyi Li**[1], **Li Liang**[5], **Dongming Sun**[1], **Shusen Zheng**[6], **Andreas Meinhardt**[7], **Wise Young**[1], **Richard Bucala**[3], and **Yi Ren**[1]

[1]W. M. Keck Center for Collaborative Neuroscience, Rutgers, The State University of New Jersey, NJ 08854, USA

[2]Statistics Laboratory, Princeton University, NJ, 08540, USA

[3]Department of Internal Medicine, Yale University School of Medicine, New Haven, CT 06520, USA

[4]Department of Anesthesiology, Xijing Hospital, The Fourth Military Medical University, Xi'an, China

[5]Department of Genetics, Rutgers, The State University of New Jersey, NJ 08854

[6]USA Department of Hepatobiliary and Pancreatic Surgery, First Affiliated Hospital, Zhejiang University, Hangzhou, China

[7]Department of Anatomy and Cell Biology, Justus-Liebig-University Giessen, Aulweg 123, D-35385 Giessen, Germany

[8]Institute of Neuroscience, The Fourth Military Medical University, Xi'an, China

[9]Department 6, Research Institute of Surgery, Daping Hospital, Third Military Medical University Chongqing, China

Abstract

The tumorigenicity of embryonic stem cells (ESCs) and induced pluripotent stem (iPS) cells is a major obstacle for clinical translation. Although teratoma formation can be reduced by *in vitro* pre-differentiation of ESCs, proliferating neural progenitors can generate tumors, especially under the immunosuppressive treatment. In our present study, we used undifferentiated embryonic stem cells as a worst-case model for teratoma formation and study if niche microenvironment of stem cell growth is a crucial driving force in teratoma development. We demonstrate herein that syngeneic ESC transplants recruit bone marrow (BM)-derived macrophages that produce macrophage migration inhibitory factor (MIF), thereby stimulating angiogenesis and teratoma development. Moreover, we show that teratoma angiogenesis relies on preexisting host endothelial cells and does not require BM-derived endothelial progenitors or endothelial cells differentiated from ESCs. Furthermore, ESCs differentiate into pericytes and pericyte coverage is restricted in MIF KO Mice. Genetic deletion of MIF from the host but not from ESCs specifically reduces angiogenesis and teratoma growth. BM cell-derived MIF contributes to teratoma development and

blockade of MIF effectively reduces teratoma development after ESC transplantation. This is the first study to demonstrate that syngeneic ESC transplantation provokes an inflammatory response that involves the rapid recruitment of BM-derived macrophages. We propose that infiltrating inflammatory macrophages form niche microenvironments that may be a crucial driving force in the initiation and progression of teratomas.

Introduction

Stem cell therapy holds an enormous potential as a treatment for many diseases, including spinal cord injury. However, embryonic stem cells (ESCs) and induced pluripotent stem (iPS) cells may produce teratomas. The risk of teratoma development represents a major obstacle to successful clinical translation of stem cell therapies. Although teratoma formation can be reduced by *in vitro* pre-differentiation of ESCs, recent observation revealed that not only undifferentiated hESCs but also ESCs proliferating neural progenitors can generate tumors (1, 2), especially under the immunosuppressive treatment (3). Teratomas have been found also after injection of *in vitro* differentiated cells into various other tissues including liver and myocardium(4–7). Human iPS cells are a potential source of patient-specific pluripotent stem cells and expected to have tremendous value for therapeutic purposes. However, it is inevitable that these iPS cells develop teratomas even if these iPS cells are pre-differentiated *in vitro* still formed teratomas (8). Furthermore, some iPS-derived neurospheres showed robust teratoma formation (9, 10). The potential tumorigenicity must be evaluated directly before the clinical application of any stem cell in regenerative medicine (11, 12).

Inflammation is a major driving force for the initiation and progression of tumor development. Macrophage migration inhibitory factor (MIF) is important in the regulation of host inflammatory and immune responses but may be recognized as a pro-tumorigenic factor (13) that is over-expressed in many tumors. We have previously shown that increased MIF expression in different cancers correlated significantly with unfavorable clinical outcomes (14–16). Given the role of MIF in inflammation and tumor development, MIF may be an important link between inflammation and teratoma development.

The tumorigenic potential of ESCs is considered to reflect a complex interactive process that requires the presence of supporting host cells. In the present study, we studied the role of the host inflammatory response in teratoma formation by syngeneic ESC transplantation. We found that ESCs recruit bone marrow (BM)-derived macrophages that deliver MIF to stimulate host endothelial cell proliferation and pericyte differentiation. We further demonstrated that MIF expressed by BM-derived macrophages is essential to teratoma growth and represents an important target to control teratoma development after ESC transplantation.

Materials and Methods

Mice strains

Wild type (WT) C57BL/6 and C57BL/6-Tg(ACTB-mRFP1)1F1Hadj/J mice "RFP mice" were purchased from Jackson Laboratory (Bar Harbor, Maine). MIF KO mice bred onto a pure C57BL/6 background (generation N10) have been described previously (17). All mice were maintained in pathogen-free animal facility at Rutgers University. Animal protocols were approved by Animal Care and Facilities Committee of Rutgers University.

Reagents and antibodies

All chemicals were purchased from Sigma (St. Louis, MO) and cell culture media were from Invitrogen (Carlsbad, CA) unless otherwise indicated. The antibody against NG2 was from Millipore (Billerica, MA) and CD31 was from BD Biosciences (Franklin Lakes, NJ). F4/80 was purchased from American Tissue Culture Collection (ATCC, Manassas, VA) and IBA-1 (ionized calcium binding adapter molecule 1) was from Wako (Osaka, Japan). A rabbit-anti-MIF antibody from Santa Cruz was used for ELISA, and a neutralizing anti-MIF IgG$_1$ monoclonal antibody (anti-MIF IgG1, source clone Monash University) was employed for the *in vivo* studies (18). The Alexa 555-conjugated goat-anti-rat IgG and HRP-conjugated goat-anti-rabbit IgG were from Invitrogen. Cy5-conjugated goat anti-rat IgG was from Novus Biologicals (Littleton, CO). Cy5-AffiniPure donkey anti-rabbit IgG was purchased from Jackson Immuno Research (West Grove, PA). The small molecule MIF antagonists ISO-1 was obtained from Calbiochem (San Diego, CA).

ESCs

Murine ESC line F12 from C57BL/6 mice ubiquitously expressing enhanced green fluorescent protein (EGFP) under the control of the chicken actin promoter (19). ESCs were cultured on a feeder free medium under an atmosphere of 5% CO_2 at 37°C. The EGFP-ESCs were maintained on 0.1% gelatin-coated dishes in ESC culture medium (ESM), which is composed of Dulbecco's modified Eagle medium (DMEM) with high glucose, 15% fetal bovine serum (FBS, Hyclone, Logan, UT), 0.1mM 2-mercaptoethanol, 1nM sodium pyruvate, 1% non-essential amino acids solution (MEM), 1% penicillin-streptomycin, 1% nucleoside solution, and 1000 U/ml murine leukemia inhibitory factor (LIF) (Chemicon, MA).

Endothelial cells

Primary lung endothelial cells were prepared from WT and MIF KO mice using CD146 MicroBeads (Miltenyi Biotec, Germany), according to the manufacturer's protocol, cultured in DMEM/F-12 containing 10% FBS, heparin sulfate (90 μg/ml), and endothelial cell growth supplement (ECGS, 450μg/ml), and used within three passages.

Mouse BM-derived macrophages (BMDM)

Mouse BM-derived macrophages (BMDM) from WT and MIF KO mice were prepared as described (20). Briefly, BM cells from mice 6–8 weeks of age were collected from femoral shafts by flushing the marrow cavity of femurs of with DMEM supplemented with 1% FBS. The cell suspensions were passed through an 18-gauge needle disperse cell clumps. Cells were cultured for 7 days at a cell density of 1×10^6/ml in 100 mm polystyrene tissue culture dishes (BD) containing in DMEM supplemented with 20% conditioned medium from L929 cells (a source of M-CSF) and 10% FBS.

Histology and immunofluorescence

Mice were transcardially perfused with 0.9% saline followed by 4% paraformaldehyde. A segment of spinal cord encompassing the transplantation site was removed and fixed in 4% paraformaldehyde for 3h and then cryoprotected in 20% sucrose overnight at 4°C. For histologic examination, the sections were stained with hematoxylin and eosin (H&E). For immunofluorescent staining, the sections were incubated with primary antibodies overnight at room temperature (RT) followed by secondary antibodies at RT for 2h. Primary antibody omission controls were performed to exclude nonspecific binding. Samples were examined and microphotographs were taken using Zeiss AxioCam microscope and AxioPhot image collection system (Carl Zeiss, Germany) and confocal Laser Scanning Microscopy (Nikon, Japan). Two to three sections containing the largest teratoma area of each mouse were used

to calculate the tumor size and positive areas using LSM 510 software (Nikon, Japan). Positive density was calculated by counting of positive areas per μm^2.

Proliferation assay

Endothelial cells and ESCs were seeded in 96-well plates at a concentration of 4000 cells and 1500 cells per well, respectively. Cells were cultured with mouse recombinant MIF, which was prepared as described by Bernhagen *et al* (21) and with an endotoxin content of <1.9EU/μg of content of protein or with culture supernatants from macrophages in the presence or absence of ISO-1. After 72 h of culture, plates were fixed with ice-cold 10% trichloroacetic acid (TCA) for 1h and stained with 0.4% sulforodamine B (SRB, w/v) in 1% v/v acetic acid for 30 min. The mean absorbance at 570 nm was measured using a Universal Microplate Reader (EL800, BIO-TEK Instruments, USA).

Transplantation of EGFP-ESCs and MIF KO ESCs

Cell density in transplantation solutions was adjusted to 10,000 viable cells per μl, and a total volume of 0.5 μl was stereotaxically injected into the spinal cord of adult WT and MIF KO mice (8–12 weeks) at T9–T10 vertebrae by a T10 laminectomy using a microliter syringe (Hamilton Company) fixed in a stereotaxi frame. Mice were allowed to be sacrificed at different time points after transplantation. Functional assessment began on post-operative 24 hrs as day 1. Hindlimb motor function was assessed using the Basso Mouse Scale (BMS) score (22).

Angiogenesis in Matrigel plugs

Recombinant mouse VEGF-A (30ng/ml, R&D Systems), heparin 60 U/ml and BSA 50μg/ml were mixed with 250 μl of regular Matrigel (BD Biosciences). The Matrigel (250 μl each) was injected subcutaneously into the abdominal region of WT and MIF KO mice as described (23). Each Matrigel plug was harvested on day 5 and fixed in 4% paraformaldehyde and then cryoprotected in 20% sucrose overnight at 4°C before being sectioned for immunohistochemistry.

Enzyme-linked immunosorbent assay (ELISA)

The supernatants of cells were collected for detection of mouse MIF by ELISA (24).

Bone marrow reconstitution

Eight week old mice as recipients were irradiated in a plastic box with 10 Gy. Subsequently, mice received an intravenous injection of 5×10^6 bone marrow cells that had been harvested by flushing the marrow cavity of femurs of appropriate donor mice with DMEM supplemented with 1% FBS. The BM cells were washed several times with PBS and then contaminating red blood cells were lysed. The BM cells were resuspended in DMEM and injected intravenously via a tail vein using a 26-gauge needle. The chimeras created by this process were defined as follows: WT   WT: WT background irradiated, reconstituted with RFP-WT bone marrow cells; WT   MIF KO: MIF KO mice irradiated, reconstituted with RFP-WT bone marrow cells; MIF KO   WT: WT mice irradiated, reconstituted with MIF KO bone marrow cells.

Treatment groups

WT mice inoculated with ESCs were randomly allocated into control and treatment groups. In the treatment groups, mice were administrated neutralizing anti-MIF mAb (20 mg/kg) or control IgG (20mg/kg) intraperitoneally every second day.

Statistical analysis

Data in figures are presented as mean ± SEM, with n representing the number of experiments. One-way analysis of variance (ANOVA) with Dunnet's multiple comparison, Wilcoxon and unpaired student t-test were used for data analysis. Statistical significance was set at P value < 0.05.

Results

Deletion of MIF from the Host but not from ESCs Inhibits Teratoma Growth

Undifferentiated EGFP-ESCs were stereotaxically injected into the spinal cord of mice exposed by a T9–T10 laminectomy. During the first week after ESCs injection, hindlimb function as reflected by the Basso mouse scale (BMS) was normal in both WT and MIF KO mice. The BMS score in WT mice decreased rapidly 10 days after injection and reached zero (paralysis). By comparison, the BMS score declined slowly after ESC injection in MIF KO mice. All WT mice were paralyzed at day 19 after cell transplantation (Figure 1A). In contrast, only one out of 14 MIF KO mice was paralyzed at day 17 (Figure 1A). We computed the rate of decay of BMS from day 8 to day 17 using the least-squares method for each mouse in both WT and MIF KO groups. The two-sided Wilcoxon test was employed to compare these rates (P<0.05). Histological examination revealed teratoma formation in the spinal cord as a cause of the hindlimb paralysis. In both WT and MIF KO mice, the tumors consisted of structures derived from all three embryonic germ lineages (Figure 1B); however, teratoma growth was significantly less pronounced in the spinal cord of MIF KO versus WT mice (Figure 1C). These data suggest that lack of host MIF is associated with reduced teratoma growth without affecting the evident pluripotency of ESCs.

We next investigated whether the genetic deletion of MIF from ESCs influenced teratoma development. MIF-deficient ESC lines were generated from the individual blastocysts of MIF KO mice. Two undifferentiated MIF-deficient ESC lines (ES4 and ES15) were injected into the spinal cords of WT mice. MIF-deficiency in ESCs did not affect teratoma development as all mice injected with these cells developed paralysis at a similar rate as those injected with WT ESCs (BMS score was 0, data not shown). Structures originating from three embryonic germ layers also were observed in MIF-deficient tumors, indicating that intrinsic MIF deficiency does not affect ESC pluripotency (Figure 1D).

Angiogenesis is Restricted in MIF KO Mice

Since angiogenesis is essential for embryonic development, we hypothesize that the rapid teratoma formation in WT mice depends on enhanced angiogenesis. ESCs were injected into the spinal cord and images were taken at 24 hrs and 2 week after cell transplantation, respectively. Figure 2A showed the ESCs grew quickly in the WT compared with those in MIF KO mice. Furthermore, newly formed blood vessels were significantly more abundant in teratomas obtained from WT mice compared to those from MIF KO mice (Figure 2A). We stained teratomas grown either in WT or MIF KO mice, for CD31, a marker of endothelial cells. Teratomas from WT mice had more blood vessels compared to those from MIF KO mice (Figure 2B). By contrast, injection of PBS alone in the spinal cord did not produce neovascularization in WT or MIK MO mice (data not shown). Blood vessel density was quantified by counting the area of vessels per unit area (μm^2) across entire teratoma sections. The ratio of vessel area/tumor area was significantly higher in teratomas from WT mice compared to teratomas from MIF KO mice (Figure 2C).

To further explore the role of MIF in neovascularization *in vivo*, MIF KO and WT mice were injected subcutaneously with Matrigel and the Matrigel plugs were excised at 5 days after implantation. Plugs from MIF KO mice were transparent, while those arising from WT

mice were reddish in color, indicating a more pronounced angiogenic response in WT mice (Figure 2D). Angiogenesis was further demonstrated by staining of the Matrigel sections with CD31 antibody. MIF KO mice exhibited a clear and significant decrease in blood vessel density when compared with WT mice (Figure 2E).

Teratoma Angiogenesis does not Require Bone Marrow (BM)-Derived EC Progenitor Cells

Confocal microcopy showed that the CD31 positive endothelial cells present in teratomas originated from the host and not from ESC differentiation, as evidenced by their negativity for GFP (Figure 3A). To assess whether the recruitment of BM-derived endothelial cells is required for teratoma growth, we lethally irradiated WT mice and transplanted red fluorescent BM cells from C57BL/6-Tg(ACTB-mRFP1)1F1Hadj/J"RFP mice". ESCs then were injected into the spinal cord of these RFP-BM reconstituted mice at 4 weeks after BM replacement. Teratomas developed after 2 weeks of ESC transplantation. The CD31$^+$ endothelial cells did not co-localize with RFP$^+$ cells in the teratoma (Figure 3B), indicating that the endothelial cells present in newly formed blood vessels were neither differentiated from ESCs nor from BM-derived cells. They were from pre-existing endothelial cell proliferation.

ESCs Differentiate into Pericytes and Pericyte Coverage is Restricted in MIF KO Mice

Angiogenesis not only requires endothelial cell proliferation but also depends on pericytes that support vessel stabilization and maturation (25). The origin of pericytes and the molecular mechanisms that regulate their differentiation are not well understood, however. We therefore assessed whether the pericytes present in the teratoma vasculature came from host tissue or from the differentiation of ESCs themselves. This was determined by expression of the pericyte marker NG2 and its localization to capillary vessels. Blood vessels in teratomas from WT mice had abundant NG2$^+$ pericytes that appeared closely apposed to the capillaries (Figure 3C). In contrast, the blood vessels in teratomas from MIF KO mice were covered only sparsely by pericytes (Figure 3C), suggesting that pericyte association with endothelium is regulated by MIF. Quantitative analysis demonstrated a significant decrease in NG2$^+$ pericyte counts in MIF KO teratomas compared to WT (Figure 3D). Furthermore, the pericyte density of vessels, as determined by the total number of pericytes divided by the density of CD31$^+$ vessels, was significantly higher in teratomas from WT mice than from MIF KO mice (Figure 3D). Moreover, NG2$^+$ pericytes in WT and MIF KO mice were derived in part from both host and the transplanted ESCs because a portion of these cells were GFP positive (Figure 3E). These results suggest that MIF plays a role in teratoma angiogenesis by regulating the recruitment/differentiation of pericytes from implanted ESCs and host cells.

We also explored whether BM is the source of the pericyte progenitors in newly formed teratoma vessels as it is accepted that BM cells give rise to pericyte precursor cells (26). ESCs were injected into the spinal cord of RFP-BM reconstituted mice at 4 weeks after BM replacement. We observed that BM-derived cells (*i.e.* RFP$^+$) were not positive for NG2 staining in teratomas from either WT or MIF KO mice (Figure 3F). Taken together, our results suggest that teratoma angiogenesis does not require BM-derived endothelial cells or pericytes and that non-BM-derived progenitors contribute to teratoma vascularization.

ESCs Recruit BM-Derived Macrophages

In tissues such as the heart, the presence of local inflammation is critical for the successful engraftment of intravenously administered ESCs (27). We therefore examined the cellular microenvironment that develops immediately after ESC implantation into spinal cords. By using the macrophage specific-markers IBA-1 and F4/80, we found macrophages in the WT spinal cords as early as the first day after ESC injection with peak macrophage infiltration

occurring after 1 to 2 weeks (Figure 4A). Notably, there was a significant reduction in macrophage infiltration when MIF-KO mice were compared to WT mice. The mean density of macrophages (IBA-1$^+$) recruited to the ESC injection site at 1 day in MIF KO mice was 0.18± 0.09 versus 2.55 ± 1.24 in WT mice (n=10, P<0.05). A similar pattern was observed at 2 weeks after ESC injection (Figure 4A, B). Both percentages of IBA-1$^+$ and F4/80$^+$ macrophages were significantly higher in WT mice compared to MIF KO mice. By contrast, surgery alone (injection of PBS) did not cause evident macrophage infiltration in both WT and MIF KO mice (data not shown).

To determine whether the macrophages within these sites represented locally activated microglia or BM-derived cell infiltration, the ESCs were injected into the spinal cord of RFP-BM reconstituted mice at 4 weeks after BM replacement and the spinal cords were examined at 2 weeks after ESC injection. Most RFP$^+$ cells were IBA-1 or F4/80 positive within the teratoma tissue, suggesting that these BM-derived cells were macrophages (Figure 4C). In other words, most IBA-1 or F4/80 positive cells co-localized with RFP$^+$ cells and we did not observe many F4/80$^+$/IBA-1$^+$ but RFP$^-$ cells in the teratomas, indicating that most macrophages in the teratomas are derived from BM-derived cells rather than locally activated microglia cells.

Macrophages Enhance Proliferation of Endothelial Cells and ESCs via Production of MIF

Macrophages are an important source of MIF (28) and our own data showed that significant macrophages infiltrated into the sites of ESC injection. We also showed that deletion of MIF from ESCs did not block teratoma development (Figure 1E). We therefore hypothesized that infiltrating macrophages deliver substantial amounts of MIF into ESC niches that then supports teratoma growth. We compared MIF production from BMDM and ESCs in vitro and observed that over a period of 48 hrs, macrophages secreted 34.63 ± 2.50 ng/ml MIF per million cells (Figure 5A), while 1.23 ± 0.06 ng/ml MIF was produced by same number ESCs. These data indicate that macrophages are a major source of MIF; accordingly, we reasoned that infiltrating macrophages may deliver MIF into ESC niches to impart a direct effect on endothelial cells or ESCs. To address this point, endothelial cells were incubated with recombinant mouse MIF (rMIF) and their proliferation was assessed. We ran the least-squares regression to see if there is a linear trend on the dose effect. The P-value was 0 with degree of freedom 47 and the multiple R^2 was 0.3484, revealing that MIF stimulates endothelial cell proliferation in a dose-dependent manner (Figure 5B). Moreover, when endothelial cells were cultured with the macrophage conditioned medium from WT or MIF KO mice, the medium from the WT macrophages caused a 90.10% ± 10.60% increase above control in endothelial cell proliferation, while medium from MIF KO macrophages did not significantly stimulate proliferation. In addition, inhibition of MIF activity by ISO-1, a small molecule inhibitor of MIF (29), by pretreatment of medium from WT macrophages significantly suppressed macrophage-induced endothelial cell proliferation (Figure 5C). We also demonstrated that rMIF and WT macrophage conditioned medium significantly enhanced proliferation of primary endothelial cells from MIF KO mice, whereas ISO-1 decreased MIF activity (Figure 5D), suggesting that cell proliferation could be rescued in the MIF KO group by the addition of rMIF. These data suggest that macrophages are a major source of the MIF that supports angiogenesis. In addition to stimulated endothelial cell proliferation, rMIF or medium from WT macrophages also enhanced ESC proliferation (Figure 5E, 5F), and inhibition of MIF by ISO-1 reduced macrophage-induced ESC proliferation (Figure 5F).

BM-Derived Cells Produce MIF that Contributes to Teratoma Angiogenesis and Growth

We showed that macrophages infiltrating into teratomas are derived from the BM and produce significant amounts of MIF that directly stimulates endothelial cell and ESC

proliferation. To better substantiate that BM-derived cells are indeed the major producer of MIF within ESC niches in vivo, ESCs were injected into the lethally irradiated MIF KO mice that had been previously re-constituted with WT BM (WT   KO mice, Figure 6A). The appearance and timing of teratoma formation in these mice were similar to that observed in fully WT host mice. Furthermore, the teratomas appeared hemorrhagic in WT   KO mice (Figure 6B) and grew significantly faster than those in the MIF KO mice that had not undergone BM transplantation (Figure 6C), suggesting that transplantation of WT BM-derived cells in MIF KO mice restored teratoma development.

We also investigated whether BM-derived cells from MIF KO mice are sufficient to suppress teratoma development by ESCs implanted into WT mice. We lethally irradiated WT mice and reconstituted their BM with either BM cells from WT (WT   WT) or MIF KO (KO   WT) mice (Figure 6A). The chimeric KO   WT mice showed decreased angiogenesis, and reduced teratoma growth when compared to chimeric WT   WT mice (Figure 6B, C). This result indicates that deletion of MIF expression in hematopoietic cells is sufficient to inhibit teratoma development. Furthermore, rMIF administration (500 μg/kg/ week, *i.p.* restored teratoma development in KO   WT mice (Figure 6D). Taken together, we conclude that BM-derived cells produce MIF that contributes to teratoma angiogenesis and growth.

Teratoma Development outside of Spinal Cord

To better exclude the effect of neighboring neural and glial cells on teratoma growth and differentiation, an examination of teratomas induced by ESC transplantation in non-neural sites could support the role of signals produced by macrophages versus other tissue types. ESCs were injected into liver and leg muscle of WT and MIF KO mice, respectively, and representative sets of teratoma that developed in each group at week 3 are shown in Figures 6E, 6F. Teratomas that developed after ESC injection were significantly smaller in the MIF KO mice compared with those in WT mice. By 3 weeks after injection, the mean teratoma size in the liver and muscle was 5.5% and 36.6% smaller in MIF KO mice than WT mice (n=8, p<0.05). These results not only confirmed that MIF is crucial for teratoma development, but also excluded the role of resident cells in the spinal cord in teratoma development.

Targeting MIF Pharmacologically Inhibits Teratoma Growth

Based on the above observations, we reasoned that selective inhibition of MIF activity would inhibit angiogenesis and teratoma growth. Mice that received an injection of ESCs were randomized into three groups. A sham group only received ESC injection without further treatment. Mice in the treatment groups were administered a neutralizing anti-MIF mAb or an isotype control antibody only by injection *i.p.* at a dose of 20 mg/kg *q.o.d.* (every other day). As shown in Figure 7A–D, mice that received anti-MIF showed a significant inhibition of blood vessel formation and teratoma progression, with a mean teratoma size of 6.88 ± 1.84 mm^3 in the anti-MIF group *vs.* 23.01 ± 5.40 mm^3 in the control IgG$_1$ group (n=8, p<0.05). Moreover, the anti-MIF treated mice teratomas had fewer numbers of CD31-positive vessels than those from the control IgG$_1$ treated mice and sham group (Figure 7D).

Discussion

Inflammatory cells play an important role in tumor progression (30). However, it is not clear whether ESCs have the potential to generate the inflammatory environment necessary for supporting their growth. This is the first study to demonstrate that syngeneic ESC transplantation provokes an inflammatory response that involves the rapid recruitment of BM-derived macrophages and alternative macrophage activation. The BM-derived

macrophages create a microenvironment that facilitates the initiation and progression of teratomas. This involves the release of MIF to promote the formation of new capillaries from preexisting vessels. Our data indicate that MIF released by BM-derived macrophages is both necessary and sufficient to drive angiogenesis and support teratoma progression, and lead to the conclusion that MIF is a key regulator in the link between inflammation and teratoma development. Although ESCs are not oncogenically transformed, they still have the ability to recruit BM-derived cells. How are these BM-derived macrophages recruited by ESCs? ESCs are known to express monocyte chemoattractant protein-1 (MCP-1 or CCL2) (31), which acts through its receptor CCR2 to induce the migration and activation of macrophages and thus tumor progression (32). Macrophage released MIF also may act as a non-canonical ligand for CXCR2 and CXCR4 (33) and further attract CXCR2$^+$ and CXCR4$^+$ macrophages, which have been shown to mediate proangiogenic effects in various models of angiogenesis (34). However, only a small portion of macrophages were CXCR4 positive during teratoma development (data not shown), suggesting that ESC-induced macrophage infiltration may be CXCR4-independent. Molecules other than chemokines also may promote monocyte recruitment. However, more detailed studies will be necessary to determine whether additional molecules either alone or in combination contribute to macrophage recruitment to the site of ESC implantation.

BM-derived cells have been shown to play an important role in tumor neovascularization and the recruitment of BM-derived endothelial and pericyte progenitors participates in tumor vascular development (35). The present study demonstrates that angiogenesis during ESC proliferation and teratoma progression does not require the contribution of BM-derived endothelial, ESC-differentiated endothelial cells or BM-derived pericyte progenitors. These results are consistent with Purhonen *et al* who observed that BM-derived cells do not contribute to vascular endothelium and are not needed for tumor growth (36). We showed that BM-derived cells directly contribute to teratoma vascular development through one major mechanism, i.e. the delivery of MIF Infiltrated macrophages produce appreciable amounts of MIF that not only regulate angiogenesis by directly interacting with endothelial cells but also enhance ESC proliferation. In addition to producing MIF, macrophages promote angiogenesis and tissue remodeling by the secretion of VEGF and metalloproteinase-9 (MMP-9) (37–39). MMP9 produced by BM-derived cells initiates the angiogenic switch leading to tumor growth and progression (37, 40, 41). It has been shown that MIF directly induces expression of MCP-1, MMP-9 and VEGF in different types of cells (16, 42). Targeting MIF may also suppress release of MCP-1, VEGF and MMP9, thereby inhibiting angiogenesis and impairing teratoma growth.

In conclusion, ESCs induce BM-derived macrophage accumulation and thus accelerate teratoma development, at least in part, by facilitating angiogenesis. Macrophage-derived MIF can directly or indirectly promote angiogenesis and thus contribute to the teratoma development. A better understanding of the regulation and function of different types of cells in the tumorigenicity of ESCs may yield useful therapies for the safe transplantation of ESCs. In addition to inhibiting MIF expression, the targeting of the host microenvironment of the transplantation site rather than ESCs directly could be a more efficient approach for suppressing angiogenesis and teratoma progression without affecting the pluripotency of ESCs. Nonsteroidal anti-inflammatory agents such as COX-2 inhibitors may be candidates for this purpose as they inhibit angiogenesis by direct effects on endothelial cells (43). MCP-1 may also be a valuable therapeutic target in teratomas as it is reported that inhibition of MCP-1 production reduces tumor angiogenesis *in vivo* (44). It is of further interest that human *MIF* is encoded by a functionally polymorphic locus (45, 46) and that *MIF* promoter polymorphisms that are associated with increased systemic MIF expression have been linked to increased clinical disease severity (46, 47). Thus, teratoma development also may have an important genetic basis that could affect the clinical selection of patients for therapy.

Acknowledgments

References

1. Roy NS, Cleren C, Singh SK, Yang L, Beal MF, Goldman SA. Functional engraftment of human ES cell-derived dopaminergic neurons enriched by coculture with telomerase-immortalized midbrain astrocytes. Nat Med. 2006; 12(11):1259–68. [PubMed: 17057709]

2. Yang D, Zhang ZJ, Oldenburg M, Ayala M, Zhang SC. Human embryonic stem cell-derived dopaminergic neurons reverse functional deficit in parkinsonian rats. Stem Cells. 2008; 26(1):55–63. [PubMed: 17951220]

3. Dressel R, Schindehutte J, Kuhlmann T, et al. The tumorigenicity of mouse embryonic stem cells and in vitro differentiated neuronal cells is controlled by the recipients' immune response. PLoS ONE. 2008; 3(7):e2622. [PubMed: 18612432]

4. Fair JH, Cairns BA, Lapaglia MA, et al. Correction of factor IX deficiency in mice by embryonic stem cells differentiated in vitro. Proc Natl Acad Sci U S A. 2005; 102(8):2958–63. [PubMed: 15699326]

5. Cao F, Lin S, Xie X, et al. In vivo visualization of embryonic stem cell survival, proliferation, and migration after cardiac delivery. Circulation. 2006; 113(7):1005–14. [PubMed: 16476845]

6. Kolossov E, Bostani T, Roell W, et al. Engraftment of engineered ES cell-derived cardiomyocytes but not BM cells restores contractile function to the infarcted myocardium. J Exp Med. 2006; 203(10):2315–27. [PubMed: 16954371]

7. Nussbaum J, Minami E, Laflamme MA, et al. Transplantation of undifferentiated murine embryonic stem cells in the heart: teratoma formation and immune response. FASEB J. 2007; 21(7):1345–57. [PubMed: 17284483]

8. Okita K, Nakagawa M, Hyenjong H, Ichisaka T, Yamanaka S. Generation of mouse induced pluripotent stem cells without viral vectors. Science. 2008; 322(5903):949–53. [PubMed: 18845712]

9. Tsuji O, Miura K, Okada Y, et al. Therapeutic potential of appropriately evaluated safe-induced pluripotent stem cells for spinal cord injury. Proc Natl Acad Sci U S A. 107(28):12704–9. [PubMed: 20615974]

10. Miura K, Okada Y, Aoi T, et al. Variation in the safety of induced pluripotent stem cell lines. Nat Biotechnol. 2009; 27(8):743–5. [PubMed: 19590502]

11. Goldring CE, Duffy PA, Benvenisty N, et al. Assessing the safety of stem cell therapeutics. Cell Stem Cell. 8(6):618–28. [PubMed: 21624806]

12. Ben-David U, Benvenisty N. The tumorigenicity of human embryonic and induced pluripotent stem cells. Nat Rev Cancer. 11(4):268–77. [PubMed: 21390058]

13. Bucala R, Donnelly SC. Macrophage migration inhibitory factor: a probable link between inflammation and cancer. Immunity. 2007; 26(3):281–5. [PubMed: 17376392]

14. Ren Y, Chan HM, Fan J, et al. Inhibition of tumor growth and metastasis in vitro and in vivo by targeting macrophage migration inhibitory factor in human neuroblastoma. Oncogene. 2006; 25(25):3501–8. [PubMed: 16449971]

15. Ren Y, Law S, Huang X, et al. Macrophage migration inhibitory factor stimulates angiogenic factor expression and correlates with differentiation and lymph node status in patients with esophageal squamous cell carcinoma. Ann Surg. 2005; 242(1):55–63. [PubMed: 15973102]

16. Ren Y, Tsui HT, Poon RT, et al. Macrophage migration inhibitory factor: roles in regulating tumor cell migration and expression of angiogenic factors in hepatocellular carcinoma. Int J Cancer. 2003; 107(1):22–9. [PubMed: 12925952]

17. Bozza M, Satoskar AR, Lin G, et al. Targeted disruption of migration inhibitory factor gene reveals its critical role in sepsis. J Exp Med. 1999; 189(2):341–6. [PubMed: 9892616]

18. Houdeau E, Moriez R, Leveque M, et al. Sex steroid regulation of macrophage migration inhibitory factor in normal and inflamed colon in the female rat. Gastroenterology. 2007; 132(3): 982–93. [PubMed: 17324399]

19. Chen J, Bernreuther C, Dihne M, Schachner M. Cell adhesion molecule l1-transfected embryonic stem cells with enhanced survival support regrowth of corticospinal tract axons in mice after spinal cord injury. J Neurotrauma. 2005; 22(8):896–906. [PubMed: 16083356]

20. Ren Y, Stuart L, Lindberg FP, et al. Nonphlogistic clearance of late apoptotic neutrophils by macrophages: efficient phagocytosis independent of beta 2 integrins. J Immunol. 2001; 166(7): 4743–50. [PubMed: 11254736]

21. Bernhagen J, Calandra T, Mitchell RA, et al. MIF is a pituitary-derived cytokine that potentiates lethal endotoxaemia. Nature. 1993; 365(6448):756–9. [PubMed: 8413654]

22. Engesser-Cesar C, Anderson AJ, Basso DM, Edgerton VR, Cotman CW. Voluntary wheel running improves recovery from a moderate spinal cord injury. J Neurotrauma. 2005; 22(1):157–71. [PubMed: 15665610]

23. Chen J, Somanath PR, Razorenova O, et al. Akt1 regulates pathological angiogenesis, vascular maturation and permeability in vivo. Nat Med. 2005; 11(11):1188–96. [PubMed: 16227992]

24. Arjona A, Foellmer HG, Town T, et al. Abrogation of macrophage migration inhibitory factor decreases West Nile virus lethality by limiting viral neuroinvasion. J Clin Invest. 2007; 117(10): 3059–66. [PubMed: 17909632]

25. Gerhardt H, Betsholtz C. Endothelial-pericyte interactions in angiogenesis. Cell Tissue Res. 2003; 314(1):15–23. [PubMed: 12883993]

26. Hall AP. Review of the pericyte during angiogenesis and its role in cancer and diabetic retinopathy. Toxicol Pathol. 2006; 34(6):763–75. [PubMed: 17162534]

27. Malek S, Kaplan E, Wang JF, et al. Successful implantation of intravenously administered stem cells correlates with severity of inflammation in murine myocarditis. Pflugers Arch. 2006; 452(3): 268–75. [PubMed: 16715295]

28. Calandra T, Bernhagen J, Mitchell RA, Bucala R. The macrophage is an important and previously unrecognized source of macrophage migration inhibitory factor. J Exp Med. 1994; 179(6):1895–902. [PubMed: 8195715]

29. Lubetsky JB, Dios A, Han J, et al. The tautomerase active site of macrophage migration inhibitory factor is a potential target for discovery of novel anti-inflammatory agents. J Biol Chem. 2002; 277(28):24976–82. [PubMed: 11997397]

30. Coussens LM, Werb Z. Inflammation and cancer. Nature. 2002; 420(6917):860–7. [PubMed: 12490959]

31. Guo Y, Graham-Evans B, Broxmeyer HE. Murine embryonic stem cells secrete cytokines/growth modulators that enhance cell survival/anti-apoptosis and stimulate colony formation of murine hematopoietic progenitor cells. Stem Cells. 2006; 24(4):850–6. [PubMed: 16339641]

32. Fujimoto H, Sangai T, Ishii G, et al. Stromal MCP-1 in mammary tumors induces tumor-associated macrophage infiltration and contributes to tumor progression. Int J Cancer. 2009; 125(6):1276–84. [PubMed: 19479998]

33. Bernhagen J, Krohn R, Lue H, et al. MIF is a noncognate ligand of CXC chemokine receptors in inflammatory and atherogenic cell recruitment. Nat Med. 2007; 13(5):587–96. [PubMed: 17435771]

34. Vandercappellen J, Van Damme J, Struyf S. The role of CXC chemokines and their receptors in cancer. Cancer Lett. 2008; 267(2):226–44. [PubMed: 18579287]

35. De Palma M, Naldini L. Role of haematopoietic cells and endothelial progenitors in tumour angiogenesis. Biochim Biophys Acta. 2006; 1766(1):159–66. [PubMed: 16857321]

36. Purhonen S, Palm J, Rossi D, et al. Bone marrow-derived circulating endothelial precursors do not contribute to vascular endothelium and are not needed for tumor growth. Proc Natl Acad Sci U S A. 2008; 105(18):6620–5. [PubMed: 18443294]

37. Coussens LM, Tinkle CL, Hanahan D, Werb Z. MMP-9 supplied by bone marrow-derived cells contributes to skin carcinogenesis. Cell. 2000; 103(3):481–90. [PubMed: 11081634]

38. Lewis JS, Landers RJ, Underwood JC, Harris AL, Lewis CE. Expression of vascular endothelial growth factor by macrophages is up-regulated in poorly vascularized areas of breast carcinomas. J Pathol. 2000; 192(2):150–8. [PubMed: 11004690]

39. Huang S, Van Arsdall M, Tedjarati S, et al. Contributions of stromal metalloproteinase-9 to angiogenesis and growth of human ovarian carcinoma in mice. J Natl Cancer Inst. 2002; 94(15): 1134–42. [PubMed: 12165638]

40. Giraudo E, Inoue M, Hanahan D. An amino-bisphosphonate targets MMP-9-expressing macrophages and angiogenesis to impair cervical carcinogenesis. J Clin Invest. 2004; 114(5):623–33. [PubMed: 15343380]

41. Ahn GO, Brown JM. Matrix metalloproteinase-9 is required for tumor vasculogenesis but not for angiogenesis: role of bone marrow-derived myelomonocytic cells. Cancer Cell. 2008; 13(3):193–205. [PubMed: 18328424]

42. Kong YZ, Yu X, Tang JJ, et al. Macrophage migration inhibitory factor induces MMP-9 expression: implications for destabilization of human atherosclerotic plaques. Atherosclerosis. 2005; 178(1):207–15. [PubMed: 15585220]

43. Jones MK, Wang H, Peskar BM, et al. Inhibition of angiogenesis by nonsteroidal anti-inflammatory drugs: insight into mechanisms and implications for cancer growth and ulcer healing. Nat Med. 1999; 5(12):1418–23. [PubMed: 10581086]

44. Loberg RD, Ying C, Craig M, et al. Targeting CCL2 with systemic delivery of neutralizing antibodies induces prostate cancer tumor regression in vivo. Cancer Res. 2007; 67(19):9417–24. [PubMed: 17909051]

45. Donn RP, Shelley E, Ollier WE, Thomson W. A novel 5 -flanking region polymorphism of macrophage migration inhibitory factor is associated with systemic-onset juvenile idiopathic arthritis. Arthritis Rheum. 2001; 44(8):1782–5. [PubMed: 11508429]

46. Baugh JA, Chitnis S, Donnelly SC, et al. A functional promoter polymorphism in the macrophage migration inhibitory factor (MIF) gene associated with disease severity in rheumatoid arthritis. Genes Immun. 2002; 3(3):170–6. [PubMed: 12070782]

47. Radstake TR, Sweep FC, Welsing P, et al. Correlation of rheumatoid arthritis severity with the genetic functional variants and circulating levels of macrophage migration inhibitory factor. Arthritis Rheum. 2005; 52(10):3020–9. [PubMed: 16200611]
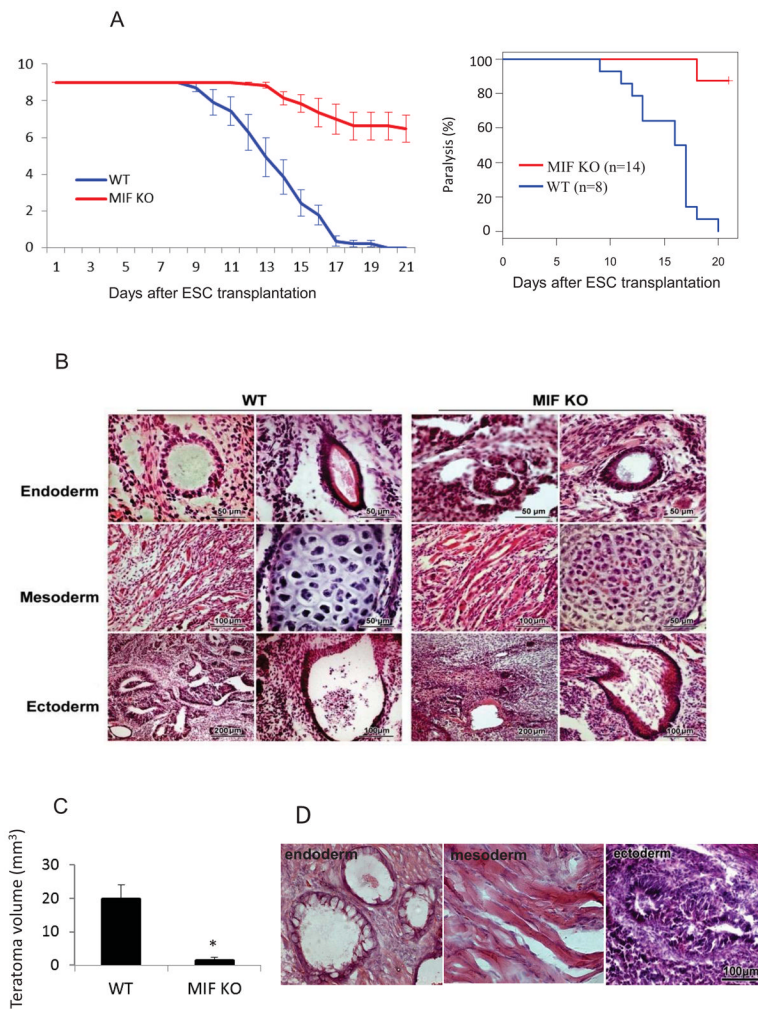
Figure 1. Deletion of MIF from the host inhibits growth of teratomas
(A) Kaplan Meier analysis was used to indicate limb paralysis in groups of WT and MIF KO mice after ESC injection in spinal cord. ESCs were stereotaxically injected into the spinal cord in WT and MIF KO mice and the function of the hindlimbs was evaluated by BMS score. A score of 0 indicates complete paralysis of the hind limbs. **(B)** Histological staining of spinal cord sections at 2 weeks after ESC injection showing structures derived from three embryonic germ lineages in both WT (left) and MIF KO mice (right). **(C)** Teratoma growth in the spinal cord from MIF KO and WT mice at 2 weeks after ESC injection (n=10, *P<0.05, two-sided Wilcoxon test). Data are represented as mean ± SEM. **(D)** HE staining of spinal cord sections at 2 weeks after injection of ESCs generated from MIF KO mice showing three embryonic structures.
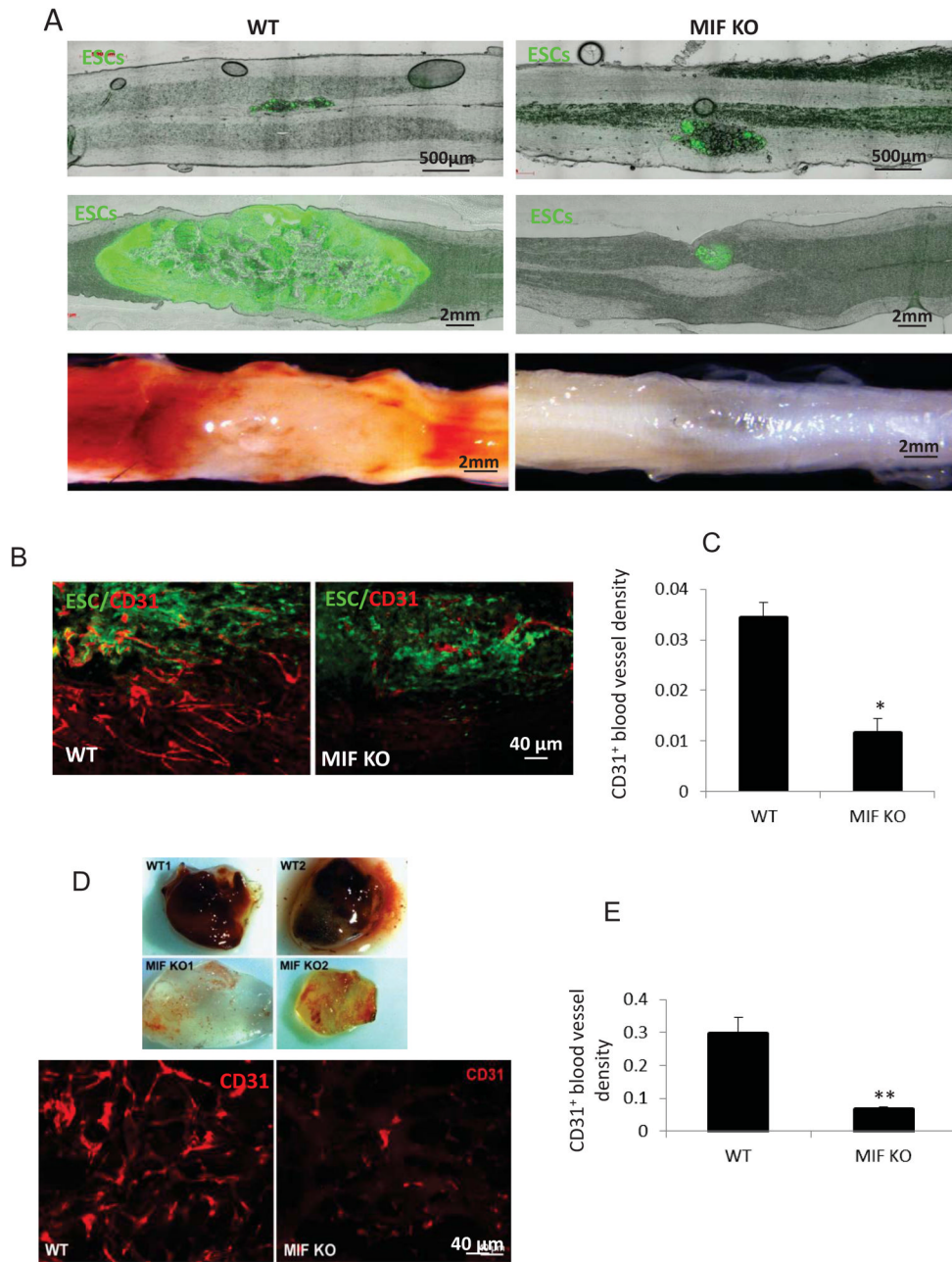
Figure 2. MIF enhances teratoma angiogenesis and development

(A) Representative micrographs showing strong EGFP expression in the spinal cord at 24 h (upper panel) and 2 weeks (middle panel) after ESC injection and the presence of associated blood vessel development at 2 weeks after ESC injection (lower panel). A representative teratoma growth from a WT mice (left panel) and MIF KO mice (right panel) is displayed. (B) Immunostaining of endothelial marker, CD31 (red) in sections from WT (left) and MIF KO mice (right) at 2 weeks after ESC injection. (C) Quantification of CD31 positive endothelial cells in teratomas from WT and MIF KO mice (n=5). (D) Representative gross morphology of Matrigel plugs (upper panel) excised 5 days postinjection in WT and MIF KO mice and CD31 staining for endothelial cells (lower panel). (E) Quantification of CD31

positive endothelial cells in Matrigel plug from WT and MIF KO mice (n=6). *p<0.05, **p<0.001, two-sided Wilcoxon test. Data are represented as mean ± SEM.
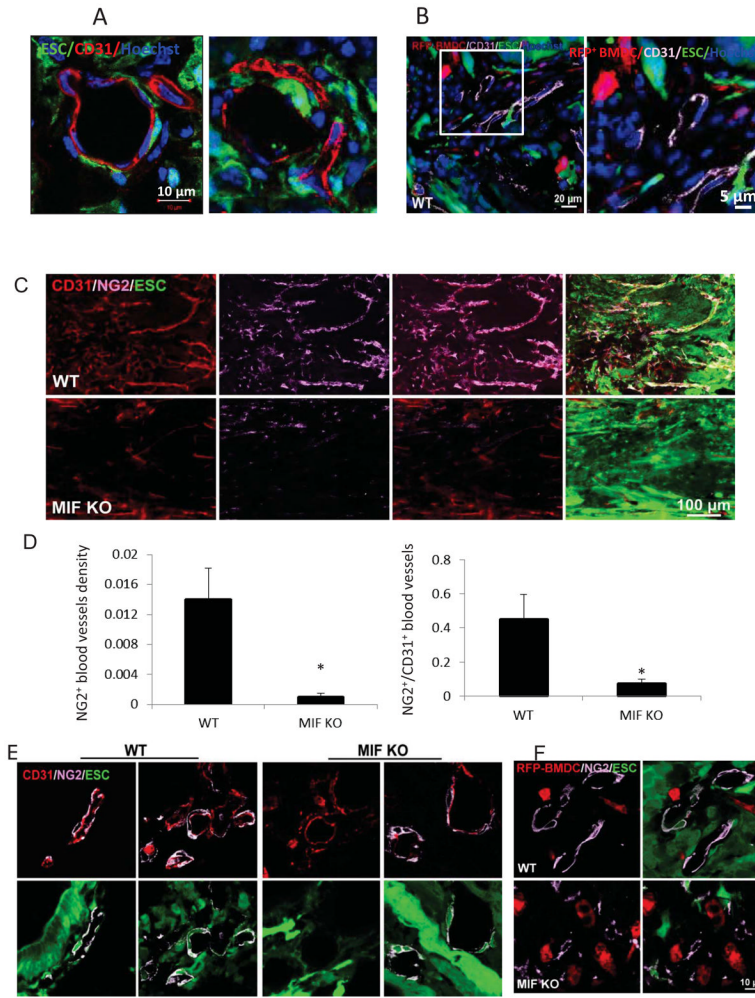
Figure 3. The origin of endothelial cells and pericytes during teratoma development in WT mice at 2 weeks after ESC injection

(A) Immunofluorescence staining for CD31 (red) using confocal microscope. **(B)** Representative photographs of immunostaining for CD31 (purple) in teratoma sections from WT mice after RFP[+] BM cell transplantation (enlarged structure on the right). **(C)** Immunostaining of sections from WT (upper panel) and MIF KO mice (lower panel) at 2 weeks after ESC injection showing double-staining for NG2 (purple) and CD31 (red). **(D)** Quantification of NG2 positive pericyte density (left), and normalized pericyte density of vessels (right, density of pericytes divided by the density of CD31^{+} vessels (n=10, *p<0.05, two-sided Wilcoxon test). Data are represented as mean ± SEM. **(E)** Representative confocal microscopic images of CD31/NG2 double-stained vessels within teratomas of WT (left panel) and MIF KO mice (right panel) at 2 weeks after ESC injection. **(F)** Representative confocal microscopic images of NG2^{+} pericytes (purple) and RFP[+] BM-derived cells (red) within teratomas of WT (upper panel) and MIF KO mice (lower panel) that received RFP[+] BM transplantation.
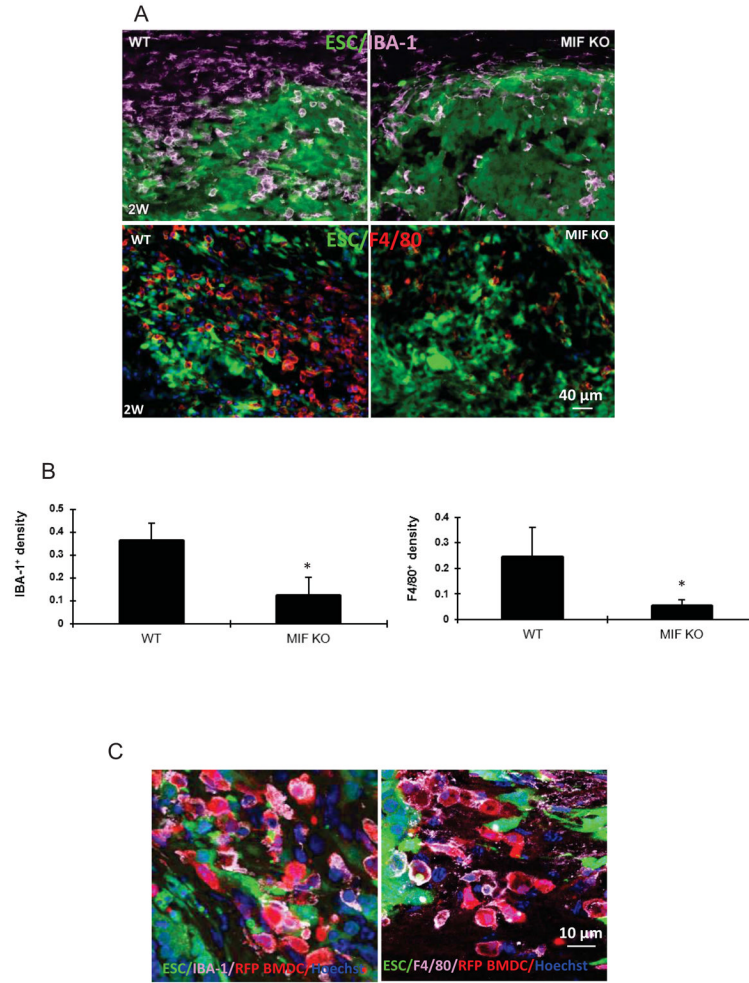
Figure 4. ESCs recruit bone marrow-derived macrophages
(A) Macrophage recruitment during teratoma progression. Macrophages in the sections of spinal cord at 2 weeks after ESC transplantation in WT (left panel) and MIF KO mice (right panel) were detected by antibodies to IBA-1 (upper panel) and F4/80 (lower panel). **(B)** Quantification of IBA-1^{+} macrophages (left) and F4/80[+] (right) at 2 weeks after ESC transplantation (n=10, *p<0.05, two-sided Wilcoxon test). Data are represented as mean ± SEM. **(C)** BM-derived macrophage recruitment during teratoma progression. Representative confocal microscopic images of sections of spinal cord from RFP-BM reconstituted mice at 2 weeks after injection were stained with IBA-1 (purple, left) and F4/80 (purple, right), respectively.
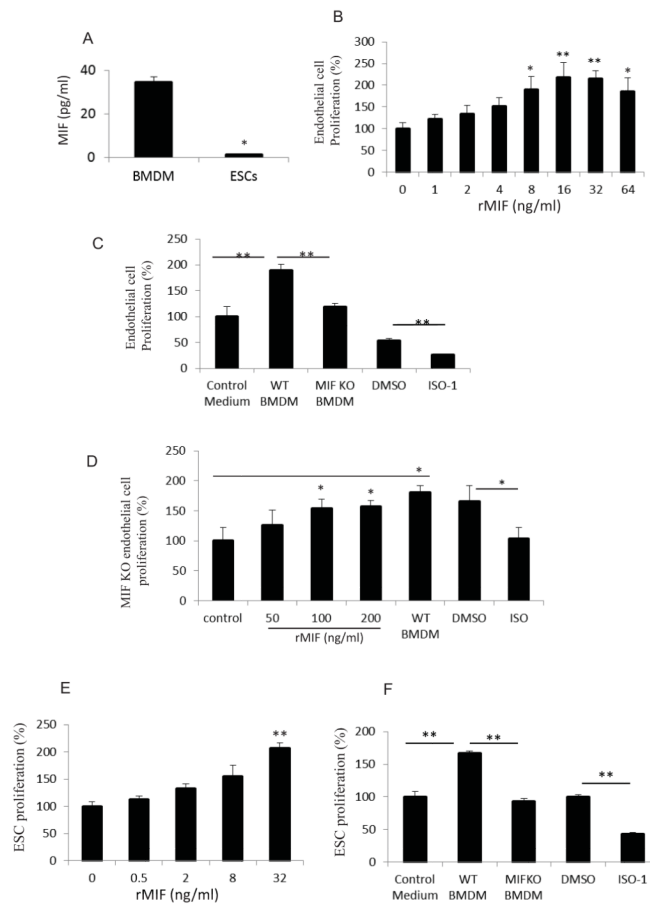
Figure 5. Macrophages enhance proliferation of endothelial cells and ESCs via production of MIF

(A) Secretion of MIF into culture supernatants of BMDM or ESCs as measured by ELISA. Supernatants were collected after 48 hrs and the values expressed as ng/ml per million cells (n=3, *p<0.05, Student's *t*-test). **(B)** Effect of MIF on endothelial cell proliferation. Endothelial cells were incubated with rMIF at the indicated concentration for 3 days and cell proliferation was assessed by SRB assay (n=3, *p<0.05, **p<0.001, ANOVA). **(C)** Effect of conditioned macrophage medium on endothelial cell proliferation. Endothelial cells were incubated with control medium, conditioned WT macrophage medium (WT BMDM), conditioned MIF KO macrophage medium (MIF KO BMDM), WT BMDM pretreated with DMSO or ISO-1 (500nM), respectively. (n=3, **p<0.001, ANOVA). **(D)** Effect of rMIF on proliferation of endothelial cell from MIF KO mice. Primary endothelial cells from MIF KO mice were incubated with rMIF, WT BMDM, WT BMDM pretreated with DMSO or ISO-1 (250nM), respectively for 3 days. (n=3, *p<0.05, ANOVA). **(E)** Effect of MIF on ESC proliferation. ESCs were incubated with rMIF at the indicated concentration for 3 days. (n=3, **p<0.001, ANOVA). **(F)** Effect of conditioned macrophage medium on ESC proliferation. ESCs were incubated with control medium, WT BMDM, MIF KO BMDM, WT BMDM pretreated with DMSO and or ISO-1 (500nM), respectively (n=3, **p<0.001, ANOVA). All data are represented as means ± SEM of three independent experiments done in duplicate.
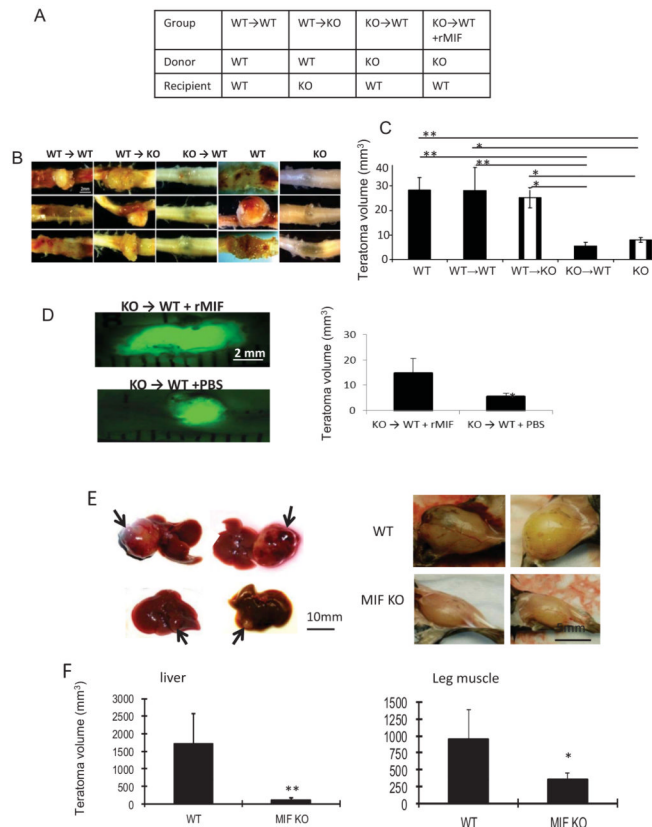
Figure 6. BM-derived cells produce MIF that contributes to teratoma growth
(A) Groups of mice used for BM reconstitution. ESCs were injected into the spinal cord in 5 groups of mice (WT, MIF KO, WT→WT, WT→KO, KO→WT). **(B)** Representative images of teratomas in the spinal cord harvested from the indicated groups at 3 weeks after ESC transplantation. **(C)** Average teratoma size at 3 weeks after ESC transplantation from the indicated groups (n=4, *p<0.05, **p<0.001, ANOVA). **(D)** rMIF or PBS were administrated into KO→WT mice and representative images of teratoma harvested from each group (left panel) and teratoma size (right) at 3 weeks after ESC transplantation (n=5, two-sided Wilcoxon test). **(E)** Representative images of teratomas in the liver (left panel, arrows) and leg muscle (right penal) at 3 weeks after ESC transplantation (1×10^6 cell/injection) in WT (upper penal) and MIF KO mice (lower penal). **(F)** Average teratoma size at 3 weeks after ESC transplantation from liver (left) and leg muscle (right) (n=8, *p<0.05, **p<0.001, two-sided Wilcoxon test).
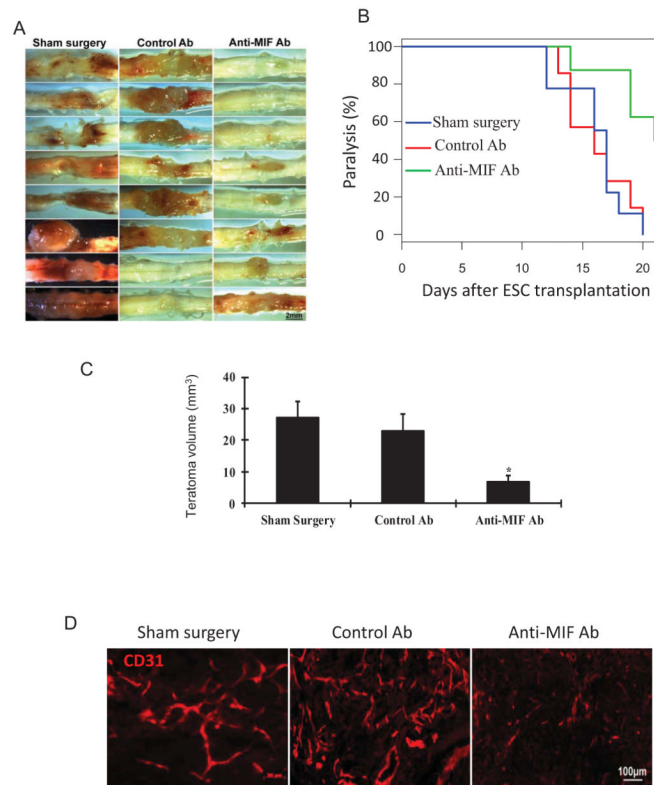
Figure 7. Targeting MIF with a neutralizing anti-MIF antibody suppresses teratoma growth
(A) Representative images of teratomas harvested from control group (sham surgery and control antibody) and treated groups (anti-MIF mAb) at 3 weeks after ESC transplantation.
(B) Kaplan Meier analysis was used to indicate limb paralysis (n=8). **(C)** Average teratoma size at 3 weeks after ESC transplantation in the indicated groups (n=8, *p<0.05, ANOVA). Data are represented as mean ± SEM. **(D)** Representative photographs of teratoma sections at 3 weeks postinjection revealing CD31 staining in sham surgery group, control antibody treated group and anti-MIF mAb treated group.